Enhanced Modulation and Noise Characteristics in 1.55μm QD Lasers Using External Optical Pumping

Maryam Sanaee and Abbas Zarifkar*

Department of Communications and Electronics, School of Electrical and Computer Engineering, Shiraz University, Shiraz, Iran
***Corresponding Author's Email:** zarifkar@shirazu.ac.ir

Received: May. 15, 2016, **Revised:** Aug. 15, 2016, **Accepted:** Sep. 7, 2016, **Available Online:** Jan. 28,2017
DOI: 10.18869/acadpub.ijop.11.1.3

ABSTRACT— The modulation response, relative intensity noise (RIN) and frequency noise (FN) characteristics of quantum dot (QD) lasers are investigated theoretically in the presence of an external optical beam. Using small signal analysis of the rate equations for carriers and photons, it is demonstrated that by injecting excess carriers into the QDs excited state through optical pumping, the modulation response of QD laser enhances and its bandwidth increases. The external optical pump also helps QD laser to turn on during shorter delay time. Further, it is deduced that the RIN level of QD laser reduces and the damping factor increases due to external beam. Moreover, the frequency noise level of QD laser and correspondingly its linewidth decreases by applying the optical beam.

KEYWORDS: Modulation bandwidth enhancement; Turn-on delay; Relative intensity noise; Frequency noise; External optical pumping; QD lasers.

I. INTRODUCTION

Self-assembled quantum dot lasers are investigated broadly since their first realization in mid 1990s, both experimentally and theoretically [1]. In fact, they are predicted to show superior characteristics which are profoundly attractive for high speed optical communications [2]-[8]. Although, recent experimental researches have demonstrated QD lasers with low threshold current at room temperature [3], high temperature stability [4]-[6], and low frequency chirping [7]-[8], the modulation response of QD lasers have shown damped relaxation oscillations with restricted bandwidth up to 10 GHz [9]-[11].

Actually, dynamic and noise properties of the laser sources are essential characteristics in communication systems. In fact, QD lasers with high modulation bandwidth help to realize isolator-free and cooler-less optical telecommunication links [12]. Moreover, having knowledge about the level of intensity and frequency noises of laser source makes it possible to estimate the transmission data rate and linewidth of the laser output under direct current modulation.

Over recent decade, considerable efforts have been devoted to investigate the main reasons of damped modulation bandwidth in QD diode lasers including carrier dynamics at different states of QD lasers or coulomb interaction [11], [13]. For instance, Wang et al. have demonstrated that the finite carrier transitions through wetting layer (WL) as well as the Pauli blocking can result in limitation of the QD laser modulation bandwidth [13]. A research report has also revealed that via band structure engineering, the dynamic characteristics of QD lasers can be tailored [14]. Several structural and technical solutions such as using tunneling injection [15], p-doping [16], two sections gain lever [17], injection locking [18], or operating at excited state emission [19] have been suggested to overcome the mentioned restrictions on the modulation bandwidth of QD lasers. One of technical suggestions for improving the

[Downloaded from ijop.ir on 2026-11-25]

modulation response of QD laser is optical locking. In this way, by injecting the laser with a tunable master laser, near to the central frequency of QD laser, its 3dB modulation bandwidth increases [18]. In fact, in optical injection locking method, an adjustable accurate and high power master laser with a frequency near to the central frequency of slave laser is needed [18].

In this paper, we suggest an alternative way to enhance the modulation response of QD lasers with the aid of a low power external optical pumping at a frequency corresponding to the excited state (ES) of QDs. By calculating the modulation response and turn-on dynamics of QD laser, it would be demonstrated that in the presence of the external optical beam, these characteristics would be improved. Moreover, it would be shown that by exploiting external optical pumping, the frequency and intensity noise properties of QD laser also enhance.

The paper is organized as follows. In section II, the theoretical modeling is described. In section III, the calculated results are presented and discussed with details. Finally, section IV contains conclusion.

II. THEORETICAL MODELING

The active region of 1.55μm QD laser is depicted schematically in Fig. 1(a). It consists of n number of InAs QD layers, deposited with surface density of $\rho=10\times10^{10}cm^{-2}$ between InP barriers. The length and width of the laser cavity are L=700μm and W=6μm, respectively. The injected carriers through electrical pumping are assumed to enter the wetting layer (WL) directly and the effect of barrier is neglected. Assuming carriers in QDs as electron-hole pairs or excitons, just dynamics of electrons in different states of conduction band are investigated. The energy diagram and the transition times of carriers are shown in Fig. 1(b). As shown, two discrete states namely as the excited state (ES) and the ground state (GS) are considered for each QDs.

In calculations, we consider an average size for all the QD ensembles and ignore the inhomogeneous size broadening of QDs. Furthermore, an external optical pumping is considered at the wavelength corresponding to the ES of QDs. An excess number of carriers are provided to the ES through absorption of the external optical beam. In practice, the spectral width of the external optical beam has to be selected similar to the homogeneous broadening of the GS in order to have high absorption efficiency at the ES. It means, we should inject excess carriers just into the ES of those QDs whose GS are contributing in lasing. On the other hand, in addition to the cascade relaxations, a direct channel for relaxation of carriers from the WL to the GS is considered for 1.55μm InAs/InP QD lasers. This assumption is based on previous experimental reports on kinetics of these kinds of QD lasers [20].

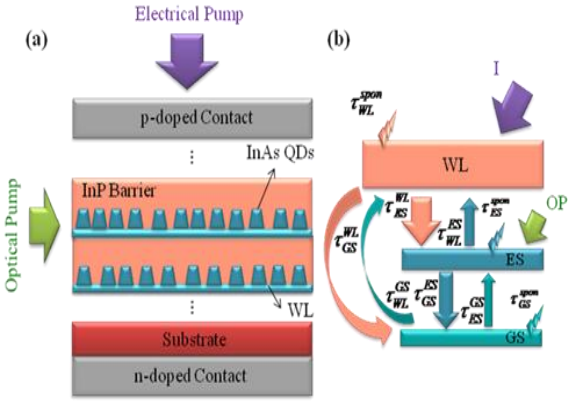

Fig. **1** (a) The schematic of 1.55μm QD laser structure (b) Carrier transition times. An excess number of carriers are provided to the ES through absorption of the external optical pump [20].

A. *Rate Equations for Carriers, Photons, and Phase*

Based on the presented flows of carriers and photons in Fig. 1(b), the following rate equations are written for the number of carriers at the WL(N_{WL}), ES(N_{ES}), GS(N_{ES}), photons (S_{GS}), [20], and phase (ϕ) [21].

$$\frac{dN_{WL}}{dt}=\frac{I}{q}-\frac{N_{WL}}{\tau_{ES}^{WL}}\left(1-\frac{N_{ES}}{4N_B}\right)-\frac{N_{WL}}{\tau_{GS}^{WL}}\left(1-\frac{N_{GS}}{2N_B}\right)+\frac{N_{ES}}{\tau_{WL}^{ES}}+\frac{N_{GS}}{\tau_{WL}^{GS}}-\frac{N_{WL}}{\tau_{WL}^{spon}} \quad (1\text{-a})$$

[Downloaded from ijop.ir on 2026-11-25]

$$\frac{dN_{ES}}{dt}=\frac{N_{WL}}{\tau_{ES}^{WL}}\left(1-\frac{N_{ES}}{4N_B}\right)+\frac{N_{GS}}{\tau_{ES}^{GS}}\left(1-\frac{N_{ES}}{4N_B}\right)-\frac{N_{ES}}{\tau_{WL}^{ES}}-\frac{N_{ES}}{\tau_{GS}^{ES}}\left(1-\frac{N_{GS}}{2N_B}\right)-\frac{N_{ES}}{\tau_{ES}^{spon}}+\underbrace{\Gamma\upsilon_g a_{ES}\left(\frac{\rho}{H_e}\right)\left(1-\frac{N_{ES}}{4N_B}\right)\left(\frac{OP}{h\upsilon_{ES}.\tau_{in}}\right)}_{External\,Optical\,Pumping} \quad (1\text{-b})$$

$$\frac{dN_{GS}}{dt}=\frac{N_{WL}}{\tau_{GS}^{WL}}\left(1-\frac{N_{GS}}{2N_B}\right)+\frac{N_{ES}}{\tau_{GS}^{ES}}\left(1-\frac{N_{GS}}{2N_B}\right)-\frac{N_{GS}}{\tau_{WL}^{GS}}-\frac{N_{GS}}{\tau_{ES}^{GS}}\left(1-\frac{N_{ES}}{4N_B}\right)-\frac{N_{GS}}{\tau_{GS}^{spon}}-\Gamma\upsilon_g a_{GS}\left(\frac{\rho}{H_e}\right)\left(\frac{N_{GS}}{N_B}-1\right)\left(\frac{S_{GS}}{1+\varepsilon_{GS}S_{GS}}\right) \quad (1\text{-c})$$

$$\frac{dS_{GS}}{dt}=\Gamma\upsilon_g a_{GS}\left(\frac{\rho}{H_e}\right)\left(\frac{N_{GS}}{N_B}-1\right)\left(\frac{S_{GS}}{1+\varepsilon_{GS}S_{GS}}\right)-\frac{S_{GS}}{\tau_P}+\beta_{sp}\frac{N_{GS}}{\tau_{GS}^{spon}} \quad (1\text{-d})$$

$$\frac{d\phi}{dt}=(\omega_L-\omega_0)+\frac{\omega_L}{n_r}\Delta n \quad (1\text{-e})$$

The parameters β_{sp}, Γ, v_g, and q show the spontaneous emission factor, the optical confinement factor, the group velocity, and the charge of an electron, respectively. The number of carriers at the GS is changed through the stimulated emission and is described by the linear gain of g_{GS} as below, while a_{GS} stands for the QD's differential gain.

$$g_{GS}=a_{GS}\left(\frac{\rho}{H_e}\right)\left(\frac{N_{GS}}{N_B}-1\right) \quad (2)$$

The term $N_B=n\rho A$ stands for the total number of QDs in the active region of the laser. The parameters A and H_e represent the area of each QD layer and the average height of QDs, respectively. The nonlinear gain coefficient is also appeared in the stimulated emission term as ε_{GS} which is normalized to the gain region volume. Moreover, due to absorption of the external optical beam photons with frequency corresponding to the ES (ν_{ES}), the number of carriers at the ES increase. As represented in equation (1-b), the number of photons which is coupled to the gain media of the laser is written as $OP/(h\nu_{ES}.\tau_{in})$, in which OP stands for the coupled optical power to the laser cavity and $\tau_{in}=2L/\upsilon_g$ denotes the round trip time in the laser cavity [22]. In fact the coupled photons are absorbed at the ES of QDs and add the number of electrons at ES through the linear gain of $\Gamma\upsilon_g a_{ES}(\frac{\rho}{H_e})(1-\frac{N_{ES}}{4N_B})$ where a_{ES} represents the differential gain at ES.

The escape rate of photons from the cavity is described by the photon lifetime τ_p and is defined as follows where α and $R_{1(2)}$ stand for the internal loss and the reflectivity of the facets, respectively.

$$\tau_p^{-1}=\upsilon_g\left(\alpha+\frac{1}{2L}\ln\left(\frac{1}{R_1R_2}\right)\right) \quad (3)$$

Two mechanisms including phonon and Auger assisted ones play essential role on the capture and relaxation times of carriers. The phonon assisted mechanism dominates at low injection currents while the Auger one becomes significant at higher pumping. Since, during the Auger recombination, the first carrier at the WL captures into the ES (GS) and transfers its energy to the second carrier at the WL, the relaxation times depend on the WL carrier number through the following relations [20].

$$\tau_{ES}^{WL}=\frac{1}{A_W+C_WN_{WL}} \quad (4\text{-a})$$

$$\tau_{GS}^{ES}=\frac{1}{A_E+C_EN_{WL}} \quad (4\text{-b})$$

The phonon and Auger assisted relaxation coefficients related to the WL (ES) are denoted as $A_W(A_E)$ and $C_W(C_E)$, respectively. Moreover, the thermal escape times of carriers under quasi Fermi equilibrium are represented as follows:

$$\tau_{ES}^{GS}=\tau_{GS}^{ES}\frac{\mu_{GS}}{\mu_{ES}}e^{\left(\frac{(E_{GS}-E_{ES})}{K_BT}\right)} \quad (5\text{-a})$$

$$\tau_{WL}^{ES}=\tau_{ES}^{WL}\frac{\mu_{ES}}{\mu_{WL}}e^{\left(\frac{(E_{WL}-E_{ES})}{K_BT}\right)} \quad (5\text{-b})$$

[Downloaded from ijop.ir on 2026-11-25]

$$\tau_{WL}^{GS} = \tau_{GS}^{WL} \frac{\mu_{GS}}{\mu_{WL}} e^{\left(\frac{(E_{WL}-E_{GS})}{K_B T}\right)} \quad (5\text{-c})$$

where E_{WL}, E_{ES}, and E_{GS} represent the resonance energies of the WL, ES, and GS, respectively. The parameters K_B and T also stand for the Boltzmann constant and the temperature. The terms of μ_{GS}, μ_{ES}, and μ_{WL} are also defined as the degeneracy of the GS, ES, and WL, respectively. Table 1 represents the definition and value of all the parameters utilized in this model, if not mentioned elsewhere. Based on the phase rate equation, the central frequency of the laser shows a finite shift above threshold due to the carrier induced refractive index changes Δn. Indeed, the phase rate equation consists of two main terms including the carriers' induced refractive index changes and the frequency shift [21]. Actually in QD lasers, besides the lasing state of the GS which produces the modal gain, two more non-lasing states of the WL and ES have essential role on overall value of the refractive index changes.

Taking into account this fact, we have calculated the frequency noise and linewidth of QD laser more precisely by considering directly the refractive index changes as a function of carriers' populations at three states of the WL, ES, and GS. In the phase rate equation (1-e), the terms ω_0 and ω_L denote the primitive frequency corresponding to λ=1.55μm and the shifted frequency (chirped frequency) of the central longitudinal mode, respectively. Two main processes such as interband transitions (IB) and free carrier absorption (FC) lead to the refractive index changes and are described in the following subsections [23].

A. *Refractive Index Changes due to interband transitions*

Based on Kramers-Kronig relation, the interband transitions of carriers at the WL, ES, and GS result into the refractive index change through the following equations [23].

$$\Delta n_{GS}^{IB} = -\frac{\Gamma c}{2\omega_0} \mu_{GS} a_{GS} \left(\frac{\rho}{H_e}\right)\left(\frac{N_{GS}}{N_B} - 1\right) = K_{GS}^{IB}\left(\frac{N_{GS}}{N_B} - 1\right) \quad (6\text{-a})$$

TABLE **1** DEFINITION AND VALUES OF NUMERICAL PARAMETERS

Symbol	Description	Value
v_g	Group velocity	8.8×10^{7} m.s^{-1}
n	Number of QD layers	5
ρ	Surface density of QDs	10×10^{14} m^{-2}
n_r	Effective refractive index of gain region	3.27
m_D^*	Effective mass of electrons in QD	0.02 m_0
m_W^*	Effective mass of electrons in WL	0.08 m_0
$\mu_{GS(ES, WL)}$	Degeneracy of QD levels and WL	2(4, 10)
Γ	Optical confinement factor at QDs	0.06
α	Average absorption coefficient	600m^{-1}
W	Width of active region	6μm
L_a	Length of cavity	1mm
β_{sp}	Spontaneous Emission Factor	10^{-4}
$\tau_{WL,ES}^{spon}$	Spontaneous Emission time at WL, ES	500ps
τ_{GS}^{spon}	Spontaneous Emission time at GS	1200ps
A_W	Auger assisted relaxation coefficients related to WL	1.35×10^{11}s^{-1}
A_E	Auger assisted relaxation coefficients related to ES	1.5×10^{11}s^{-1}
C_W	Phonon assisted relaxation coefficients at WL	5×10^{-14}s^{-1}
C_E	Phonon assisted relaxation coefficients at ES	9×10^{-13}s^{-1}
$R_{1(2)}$	Facets reflectivities	0.33
T	Device temperature	300k
H_e	Average height of QDs	2nm
$E_{WL,ES,GS}$	Emission energies related to WL, ES, GS	1.05, 0.87, 0.8eV
$a_{GS(ES)}$	QDs differential gain	5×10^{-14}m^{-1}
ε_0	Vacuum Permittivity	8.85×10^{-12}F.m^{-1}
K_B	Boltzmann constant	8.62×10^{-5}eV.k^{-1}
T	Device temperature	300k
ε_{GS}	Nonlinear gain	1×10^{-7}

[Downloaded from ijop.ir on 2026-11-25]

$$\Delta n_{ES}^{IB} = -\frac{\Gamma c}{2\omega_0}\mu_{ES}a_{GS}\left(\frac{\rho}{H_e}\right)\left(\frac{N_{ES}}{2N_B}-1\right) = K_{ES}^{IB}\left(\frac{N_{ES}}{2N_B}-1\right) \quad (6\text{-b})$$

$$\Delta n_{WL}^{IB} = -\frac{\Gamma_W c}{2\omega_0}\mu_{WL}a_{GS}\left(\frac{\rho}{H_e}\right)\left(\frac{2N_{WL}}{\mu_{WL}N_B}-1\right) = K_{WL}^{IB}\left(\frac{2N_{WL}}{\mu_{WL}N_B}-1\right) \quad (6\text{-c})$$

B. *Refractive index changes due to free carriers absorption*

Moreover, the plasma effect leads to refractive index change through free carrier absorption from the WL, ES, and GS and can be described by Drude model [23].

$$\Delta n_{GS}^{FC} = -\frac{\Gamma q^2}{n_r\varepsilon_0 m_D^* \omega_0^2}\left(\frac{\rho}{H_e}\right)\frac{N_{GS}}{N_B} = K_{GS}^{FC}N_{GS} \quad (7\text{-a})$$

$$\Delta n_{ES}^{FC} = -\frac{\Gamma q^2}{n_r\varepsilon_0 m_D^* \omega_0^2}\left(\frac{\rho}{H_e}\right)\frac{N_{ES}}{N_B} = K_{ES}^{FC}N_{ES} \quad (7\text{-b})$$

$$\Delta n_{WL}^{FC} = -\frac{\Gamma q^2}{n_r\varepsilon_0 m_W^* \omega_0^2}\left(\frac{\rho}{H_e}\right)\frac{N_{WL}}{N_B} = K_{WL}^{FC}N_{WL} \quad (7\text{-c})$$

Then, by summing up the IB and FC index changes, the total refractive index change is calculated.

B. *Small Signal Modulation Response*

In order to obtain the modulation response, we assume a sinusoidal small signal modulation term for injected current which in turn leads to modulations of the carriers, photons, and phase as follows:

$$n_i(t) = N_i + \delta n_i(t)\ ;\ i = WL, ES, GS \quad (8\text{-a})$$

$$s_{GS}(t) = S_{GS} + \delta s_{GS}(t) \quad (8\text{-b})$$

$$\phi(t) = \phi_0 + \delta\varphi(t) \quad (8\text{-c})$$

The terms $\delta n_i(t)$, $\delta s_{GS}(t)$, and $\delta\varphi(t)$ show the small signal modulations of the carriers, photons, and phase, respectively. Using Runge-Kutta method, the steady state values for number of the carriers (N_i), photons (S_{GS}) and the central frequency (ω_L) are calculated under pumping current of I and pumping light power of OP. The small signal terms of the rate equations are linearized by neglecting higher powers of the modulations as follows, where the dot sign above the variables denotes the time derivative.

$$\dot{\delta n}_{WL} = \frac{\delta i(t)}{q} - \frac{\delta n_{WL}}{\tau_{ES}^{WL}}\left(1-\frac{N_{ES}}{4N_B}\right) - \frac{\delta n_{WL}}{\tau_{WL}^{spon}} + \frac{\delta n_{ES}}{\tau_{WL}^{ES}} - \frac{\delta n_{WL}}{\tau_{GS}^{WL}}\left(1-\frac{N_{GS}}{2N_B}\right) + \frac{N_{WL}}{\tau_{ES}^{WL}}\left(\frac{\delta n_{ES}}{4N_B}\right) + \frac{\delta n_{GS}}{\tau_{WL}^{GS}} + \frac{N_{WL}}{\tau_{GS}^{WL}}\left(\frac{\delta n_{GS}}{2N_B}\right) \quad (9\text{-a})$$

$$\dot{\delta n}_{ES} = \frac{\delta n_{WL}}{\tau_{ES}^{WL}}\left(1-\frac{N_{ES}}{4N_B}\right) - \frac{N_{WL}}{\tau_{ES}^{WL}}\left(\frac{\delta n_{ES}}{4N_B}\right) - \frac{\delta n_{ES}}{\tau_{WL}^{ES}} - \frac{\delta n_{ES}}{\tau_{GS}^{ES}}\left(1-\frac{N_{GS}}{2N_B}\right) - \frac{\delta n_{ES}}{\tau_{ES}^{spon}} - \frac{N_{GS}}{\tau_{ES}^{GS}}\left(\frac{\delta n_{ES}}{4N_B}\right) + \frac{\delta n_{GS}}{\tau_{ES}^{GS}}\left(1-\frac{N_{ES}}{4N_B}\right) + \frac{N_{ES}}{\tau_{GS}^{ES}}\left(\frac{\delta n_{GS}}{2N_B}\right) \underbrace{- \Gamma\upsilon_g a_{ES}\left(\frac{\rho}{H_e}\right)\left(\frac{OP}{h\upsilon_{ES}}\right)\left(\frac{\delta n_{ES}}{4N_B}\right)}_{External\ Optical\ Pumping} \quad (9\text{-b})$$

$$\dot{\delta n}_{GS} = \frac{\delta n_{WL}}{\tau_{GS}^{WL}}\left(1-\frac{N_{GS}}{2N_B}\right) - \frac{\delta n_{GS}}{\tau_{WL}^{GS}} + \frac{\delta n_{ES}}{\tau_{GS}^{ES}}\left(1-\frac{N_{GS}}{2N_B}\right) - \frac{N_{ES}}{\tau_{GS}^{ES}}\left(\frac{\delta n_{GS}}{2N_B}\right) - \Gamma\upsilon_g a_{GS}\left(\frac{\rho}{H_e}\right)\left(\frac{\delta n_{GS}}{N_B}\right)\frac{S_{GS}}{1+\varepsilon S_{GS}} - \Gamma\upsilon_g a_{GS}\left(\frac{\rho}{H_e}\right)\left(\frac{N_{GS}}{N_B}-1\right)\frac{\delta s_{GS}}{(1+\varepsilon S_{GS})^2} - \frac{\delta n_{GS}}{\tau_{GS}^{spon}} \quad (9\text{-c})$$

$$\dot{\delta s}_{GS} = \Gamma\upsilon_g a_{GS}\left(\frac{\rho}{H_e}\right)\left(\frac{\delta n_{GS}}{N_B}\right)\frac{S_{GS}}{1+\varepsilon S_{GS}} - \frac{\delta s_{GS}}{\tau_P} + \Gamma\upsilon_g a_{GS}\left(\frac{\rho}{H_e}\right)\left(\frac{N_{GS}}{N_B}-1\right)\frac{\delta s_{GS}}{(1+\varepsilon S_{GS})^2} + \beta_{sp}\frac{\delta n_{GS}}{\tau_{GS}^{spon}} \quad (9\text{-d})$$

A closed form as a single matrix equation can be obtained after taking Fourier transform of the above small signal rate equations.

[Downloaded from ijop.ir on 2026-11-25]

$$\sum_{l=1}^{4}[a_{ml}(\omega)]_{4\times4}.\left[\delta\tilde{n}_l(\omega)\right]_{4\times1}=\left[\delta\tilde{i}(\omega),0,0,0\right]^T_{4\times1}$$
$$m,l=WL,ES,GS,and\ S \quad (10)$$

The term $[a_{ml}]_{4\times4}$ denotes the coefficients matrix of the linear small signal rate equations (9-a) to (9-d). The modulation transfer function of QD laser ($IM(\omega)$) under external optical pumping can be obtained as:

$$IM(\omega)=\frac{\delta\tilde{s}_{GS}(\omega)}{\left(\delta\tilde{i}(\omega)/q\right)}=\frac{Det_1^4(\omega)}{H(\omega)} \quad (11)$$

$H(\omega)$ is the determinant of the small signal matrix and the term Det_m^i stands for the determinant of the coefficients matrix $[a_{ml}]_{4\times4}$ in which its *i*-th column is replaced by a vector matrix $[V_m]_{4\times1}$. This vector matrix has zero elements except the *m*-th one, which is equal to one.

C. *Correlation coefficients and Noise Characteristics*

In order to calculate the frequency and relative intensity noise characteristics of QD laser, the Langevin noise sources associated to the WL, ES, GS carriers, photons and phase (F_{WL}, F_{ES}, F_{GS}, F_S, and F_ϕ) are added to the main and small signal rate equations. Furthermore, time dependent fluctuations are considered for all the variables similar to the modulation terms in equations (8-a) to (8-c). In noise calculations, the set of small signal rate equations are similarly represented in a single matrix relation by taking Fourier transform.

$$\sum_{l=1}^{4}[a_{ml}(\omega)]_{4\times4}.[\tilde{\delta n}_l(\omega)]_{4\times1}=[\tilde{F}_m(\omega)]_{4\times1}\ ;$$
$$m,l=WL,ES,GS,and\ S \quad (12)$$

Here, the terms $\tilde{F}_m(\omega)$ and $\tilde{\delta n}_l(\omega)$ stand for the Fourier transform of the corresponding Langevin noise sources and the fluctuations of the carriers or photons, respectively, in frequency domain ω. The system does not show memory and Langevin noise sources satisfy the following relations under Markovian assumptions [24]:

$$\langle F_k(t)\rangle=0 \quad (13\text{-a})$$

$$\langle F_k(t)F_{k'}(t')\rangle=2D_{kk'}\delta(t-t') \quad (13\text{-b})$$

The ensemble average and the correlation coefficients between noise sources are denoted as the angel brackets $\langle * \rangle$ and $D_{kk'}$, respectively. Since, each of the discrete random processes of carriers' or photons' flows into or out of a state or lasing mode contributes to shot noise, the auto correlation strength of D_{kk} are calculated by summing over all the particles' flows into or out of the reservoir [25]:

$$2D_{WW}=2\left(\frac{N_{WL}}{\tau_{ES}^{WL}}\left(1-\frac{N_{ES}}{4N_B}\right)+\frac{N_{WL}}{\tau_{GS}^{WL}}\left(1-\frac{N_{GS}}{2N_B}\right)+\frac{N_{WL}}{\tau_{WL}^{spon}}+\frac{N_{ES}}{\tau_{WL}^{ES}}+\frac{N_{GS}}{\tau_{WL}^{GS}}\right) \quad (14\text{-a})$$

$$2D_{EE}=2\left(\frac{N_{WL}}{\tau_{ES}^{WL}}\left(1-\frac{N_{ES}}{4N_B}\right)+\frac{N_{ES}}{\tau_{WL}^{ES}}+\frac{N_{ES}}{\tau_{ES}^{spon}}+\frac{N_{ES}}{\tau_{GS}^{ES}}\left(1-\frac{N_{GS}}{2N_B}\right)+\frac{N_{GS}}{\tau_{ES}^{GS}}\left(1-\frac{N_{ES}}{4N_B}\right)+\underbrace{\Gamma\upsilon_g a_{ES}\left(\frac{\rho}{H_e}\right)\left(1-\frac{N_{ES}}{4N_B}\right)\left(\frac{OP}{h\upsilon_{ES}}\right)}_{External\ Optical\ Pumping}\right) \quad (14\text{-b})$$

$$2D_{GG}=2\left(\Gamma\upsilon_g a_{GS}\left(\frac{\rho}{H_e}\right)\left(\frac{N_{GS}}{N_B}-1\right)\frac{S_{GS}}{1+\varepsilon S_{GS}}+\frac{N_{WL}}{\tau_{GS}^{WL}}\left(1-\frac{N_{GS}}{2N_B}\right)+\frac{N_{ES}}{\tau_{GS}^{ES}}\left(1-\frac{N_{GS}}{2N_B}\right)+\frac{N_{GS}}{\tau_{WL}^{GS}}+\frac{N_{GS}}{\tau_{GS}^{spon}}\right) \quad (14\text{-c})$$

$$2D_{SS}=2\left(\Gamma\upsilon_g a_{GS}\left(\frac{\rho}{H_e}\right)\left(\frac{N_{GS}}{N_B}-1\right)\frac{S_{GS}}{1+\varepsilon S_{GS}}+\frac{S_{GS}}{\tau_P}+\beta_{sp}\frac{N_{GS}}{\tau_{GS}^{spon}}\right) \quad (14\text{-d})$$

So long as a state or a lasing mode gains a particle ($F_k>0$), the other reservoir would

[Downloaded from ijop.ir on 2026-11-25]

lose a particle ($F_{k'}<0$). Therefore, each pair of different noise sources are correlated negatively and the cross correlation coefficients $D_{kk'}$ are calculated by summing up the flows of carriers or photons which affect both reservoirs simultaneously [25]:

$$D_{WE}=-\left(\frac{N_{WL}}{\tau_{ES}^{WL}}\left(1-\frac{N_{ES}}{4N_B}\right)+\frac{N_{ES}}{\tau_{WL}^{ES}}\right) \quad (15\text{-a})$$

$$D_{WG}=-\left(\frac{N_{WL}}{\tau_{GS}^{WL}}\left(1-\frac{N_{GS}}{2N_B}\right)+\frac{N_{GS}}{\tau_{WL}^{GS}}\right) \quad (15\text{-b})$$

$$D_{EG}=-\left(\frac{N_{ES}}{\tau_{GS}^{ES}}\left(1-\frac{N_{GS}}{2N_B}\right)+\frac{N_{GS}}{\tau_{ES}^{GS}}\left(1-\frac{N_{ES}}{4N_B}\right)\right) \quad (15\text{-c})$$

$$D_{GS}=-\Gamma\upsilon_g a_{GS}\left(\frac{\rho}{H_e}\right)\left(\frac{N_{GS}}{N_B}-1\right)\frac{S_{GS}}{1+\varepsilon S_{GS}} \quad (15\text{-d})$$

Moreover, since just the GS carriers have contribution in the formation of photons, two cross correlation coefficients of D_{WS} and D_{ES} are equal to zero.

C. *Relative Intensity Noise*

The output power of QD laser fluctuates randomly around its operation point. Using a photo detector with a wide bandwidth of Δf along with a spectrum analyzer, aforementioned fluctuations could be detected in frequency domain. Such measurements yield the noise spectrum regarded to the laser output power. Thus, the intensity noise is characterized by the relative intensity noise per unit bandwidth as following [24]:

$$\frac{RIN}{\Delta f}=\frac{S_p(\omega)}{{S_{GS}}^2} \quad (16)$$

Under ergodic stochastic assumptions, the ensemble average can be replaced by a time average over interval T. The spectral density of $S_p(\omega)=\int_{-\infty}^{+\infty}\langle\delta s_{GS}(t+\tau)\delta s_{GS}(t)\rangle\exp(-i\omega t)d\tau$ is related to $\tilde{\delta}s_{GS}(\omega)$ as follows [24]:

$$S_p(\omega)=\lim_{T\to\infty}\frac{1}{T}\int_{-\frac{T}{2}}^{\frac{T}{2}}\tilde{\delta}s_{GS}(\omega)\tilde{\delta}{s_{GS}}^*(\omega)d\tau =|\tilde{\delta}s_{GS}(\omega)|^2 \quad (17)$$

By solving the matrix equation (12), the total spectrum of photon fluctuations is calculated [22]:

$$\tilde{\delta}s_{GS}(\omega)=\frac{\sum_{m=1}^{4}Det_m^4(\omega)\tilde{F}_m(\omega)}{H(\omega)} \quad (18)$$

Now $RIN(\omega)$ is evaluated from the defined functions while the term '*Re*' represents the real part.

$$\frac{RIN(\omega)}{\Delta f}=\frac{1}{{S_{GS}}^2|H(\omega)|^2}\left(\sum_{m=1}^{4}2D_{m,m}|Det_m^4|^2+\sum_{l=1}^{4}\sum_{m=1}^{4}2D_{m,l}\,\mathrm{Re}\left(Det_m^4.Det_m^{4*}\right)\right) \quad (19)$$

D. *Frequency Noise*

For studying the phase related correlation coefficients, the electric field of optical beam is investigated. Actually, the electric field consists of both in-phase and out-phase fluctuations as illustrated in complex plane in Fig. 2.

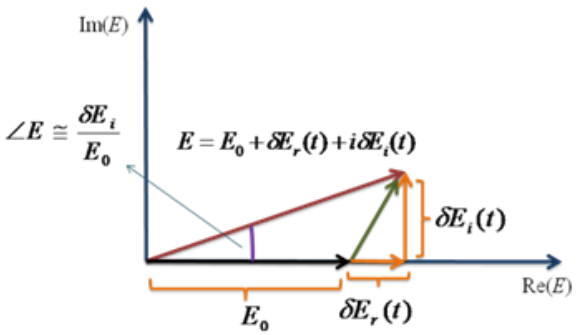

Fig. **2** Vector illustration of the relationship between the instantaneous field magnitude and the in-phase and out-phase noise components [25].

Denoting the in-phase and out-phase random fields by $\delta E_r(t)$ and $\delta E_i(t)$, respectively, the total instantaneous field and associated

[Downloaded from ijop.ir on 2026-11-25]

complex Langevin noise source $F_E(t)$ are related as follows [26]:

$$E(t) = E_0 + \delta E_r(t) + i\delta E_i(t) \quad (20\text{-a})$$

$$F_E(t) = F_r(t) + iF_i(t) \quad (20\text{-b})$$

The terms $F_r(t)$ and $F_i(t)$ stand for the in-phase and out-phase noise sources of the optical field, respectively. Thus, the Langevin noise sources of the photon and phase are related to the in-phase and out-phase fluctuations as depicted in Fig. 2 [26, 27]. It is assumed that $\delta E_r(t)$ and $\delta E_i(t)$ are much smaller than E_0.

$$E^* E \cong E_0^2 + 2E_0\delta E_r \quad (21\text{-a})$$

$$\angle E \cong \frac{\delta E_i}{E_0} \quad (21\text{-b})$$

In equation (21-a), the term E_0^2 is equivalent to the average photon number at operation point, S_{GS}, and the term $2E_0\delta E_r$ stands for the photon number fluctuation, $F_S(t)$. The term $\angle E$ also can be replaced with the phase fluctuation $F_\phi(t)$ as follows:

$$F_S(t) \cong 2\sqrt{S_{GS}}F_r(t) \quad (22\text{-a})$$

$$F_\varphi(t) \cong \frac{F_i(t)}{\sqrt{S_{GS}}} \quad (22\text{-b})$$

We can obtain the following relations by assuming equal spectral density for both in-phase and out-phase field fluctuations.

$$\langle F_r F_r \rangle = \frac{1}{4S_{GS}}\langle F_S F_S \rangle \quad (23\text{-a})$$

$$\langle F_\varphi F_\varphi \rangle = \frac{1}{S_{GS}}\langle F_i F_i \rangle = \frac{1}{4S_{GS}^2}\langle F_S F_S \rangle \quad (23\text{-b})$$

Since the phase fluctuation is the secondary effect of the carriers and photon noises, the phase Langevin source is uncorrelated to the carrier and photon noise sources and so the cross correlation coefficients $\langle F_\varphi F_S \rangle$ and $\langle F_\varphi F_{WL(ES,GS)} \rangle$ are equal to zero. We know that the phase variations lead to frequency fluctuation through the relation $2\pi\delta\upsilon_L = \delta\dot{\varphi}(t)$. Therefore, by taking ensemble average of $\delta\dot{\varphi}(t)$, we can calculate the spectral density of the frequency noise [26, 27]:

$$FN(\omega) = \frac{1}{4\pi^2}\int_{-\infty}^{+\infty}\left\langle \delta\dot{\varphi}(t+\tau)\delta\dot{\varphi}(t)\right\rangle e^{(-i\omega\tau)}d\tau \quad (24)$$

Similar to RIN, the spectral density of the frequency noise can be obtained simply by considering the noise fluctuations as ergodic stochastic processes [27].

$$FN(\omega) = \frac{1}{4\pi^2}\left\langle \left|\omega\delta\tilde{\varphi}(\omega)\right|^2 \right\rangle \quad (25)$$

The term $\delta\tilde{\varphi}(\omega)$ represents the Fourier transform of the phase fluctuation and is calculated by the small signal rate equation for the phase in the modulation frequency domain.

$$i\omega\delta\tilde{\varphi}(\omega) = \frac{\omega_L}{n_r}\delta(\Delta\tilde{n}(\omega)) + \tilde{F}_\varphi(\omega) \quad (26)$$

Here, $\delta(\Delta\tilde{n}(\omega))$ denotes the Fourier transform of the small signal fluctuations of the refractive index changes and can be calculated versus the carrier fluctuations.

$$\delta(\Delta\tilde{n}(\omega)) = \sum_{i=WL,ES,GS}(K_i^{IB} + K_i^{FC})\delta\tilde{n}_i(\omega) \quad (27)$$

Each of the carrier fluctuations $\delta\tilde{n}_i(\omega)$ can be calculated as a function of four Langevin noise sources of the carriers and photons based on equation (12). After some manipulation, we can derive the frequency noise as following whereas the terms FN_m and $FN_{m,l}$ (m, l=WL, ES, GS), stand for the self-frequency noises from each of the carrier states and the mutual frequency noises from each pair of them, respectively.

[Downloaded from ijop.ir on 2026-11-25]

$$FN(\omega)=\frac{1}{4\pi^2}\left(FN_{GS}+FN_{ES}+FN_{WL}+2FN_{WL,ES}+2FN_{WL,GS}+2F_{ES,GS}\right)+\frac{1}{16\pi^2 S_{GS}{}^2}D_{SS} \quad (28)$$

For instance, the closed forms for one of the self and mutual frequency noises are given below.

$$FN_{ES}=\frac{1}{\left(H(\omega)H^*(\omega)\right)}\times\left[\sum_{m=1}^{4}D_{m,m}\,|Det_m^2|^2+\sum_{l=1}^{4}\sum_{m=1}^{4}D_{m,l}\,\mathrm{Re}\left(Det_l^2 Det_m^{2*}\right)\right] \quad (29)$$

$$FN_{ES,GS}=\frac{1}{\left(H(\omega)H^*(\omega)\right)}\times\left[\sum_{m=1}^{4}D_{m,m}\,\mathrm{Re}[Det_m^3 Det_m^{2*}\right]+\sum_{l=1}^{4}\sum_{m=1}^{4}D_{m,l}\,\mathrm{Re}\left[Det_l^3 Det_m^{2*}\right] \quad (30)$$

In the following section, we would present the calculated results based on the aforementioned theoretical modeling. We discuss about the effect of external optical pumping on enhanced modulation response, the frequency noise and the relative intensity noise characteristics of 1.55μm QD lasers.

III. Results and Discussion

To study the impacts of external optical pumping on the modulation and noise characteristics of 1.55μm QD lasers, first we have calculated the steady state number of carriers and photons at different optical pump powers and under constant injection current. In Fig. 3(a), the carrier numbers at the WL, ES, and GS are plotted versus injection current at two optical pump power values.

As depicted, external optical beam causes the number of carriers at the GS to reach its final value at lower bias point which leads to lower threshold current. By increasing the power of the optical pump to the values more than 2.5 mW, the threshold current becomes zero. Moreover, the number of carriers at the ES grows slightly due to external optical beam by providing excess carriers to this state. On the other hand, the WL carrier number remains unchanged as long as we have bypassed the WL state by injecting carriers to the ES directly via optical beam. In Fig. 3(b), the light-current characteristics of the laser are also depicted for three different optical pump powers. It is revealed that external optical beam increases the output power. In fact, by providing excess carriers to the ES and hence the GS, the rate of stimulated emission grows under optical pumping.

The modulation response of QD laser has been evaluated using the above theoretical model for three different values of optical pump powers and is shown in Fig. 4 for an injection current of 55mA. From this figure, it is deduced that by increasing the external optical pumping, the modulation response of QD laser gets wider and its 3dB bandwidth increases.

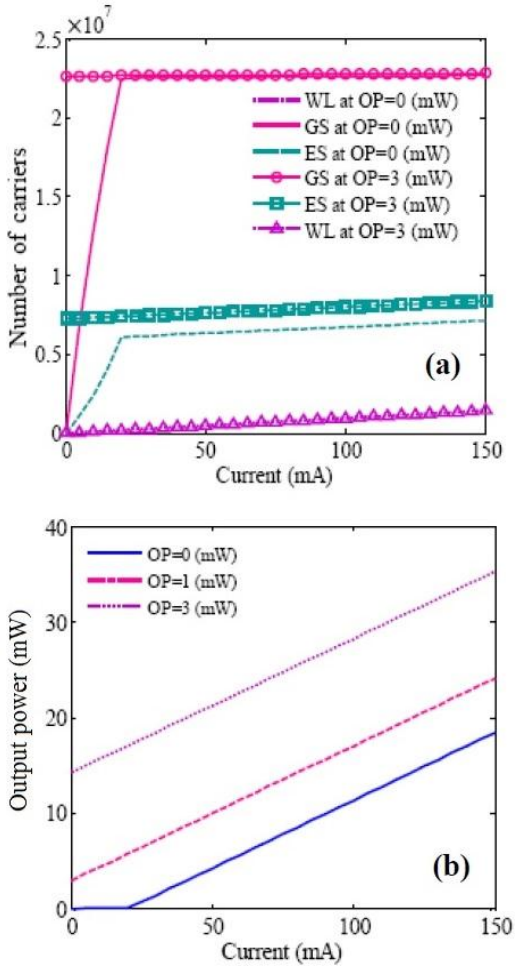

Fig. 3 (a) Number of carriers at the WL, ES, and GS versus current at two different optical pump powers. (b) Light-current characteristics of QD laser for three different optical pump powers.

[Downloaded from ijop.ir on 2026-11-25]

In fact, by injecting external carriers directly to the ES, the relaxation and escape times would not vary since the population of the WL carriers remains unchanged. But the rate of carrier flows between the ES and GS increases due to increase of carrier numbers at the ES. Therefore, the photon generation process via stimulated emission can follow the modulated injected current at higher frequencies because of the excess carriers provided to the GS. Consequently, the 3dB bandwidth of QD laser would increase by pumping the laser with an external beam. On the other hand, as shown in Fig. 4, the gain nonlinearity restricts the modulation bandwidth of QD laser at higher optical pumping. Actually, due to gain compression effects, external optical pumping saturates the GS carriers and stops increasing the 3dB modulation bandwidth [25, 27].

To get clear insight into the effect of optical pumping, we have plotted the 3dB bandwidth of QD laser versus current and optical pump power in Fig. 5. As demonstrated, by pumping QD laser with an external optical beam, we can modulate the laser electrically at lower bias currents with higher frequencies up to 14.5GHz. Meanwhile, without external optical beam, QD laser can be modulated up to 9 GHz.

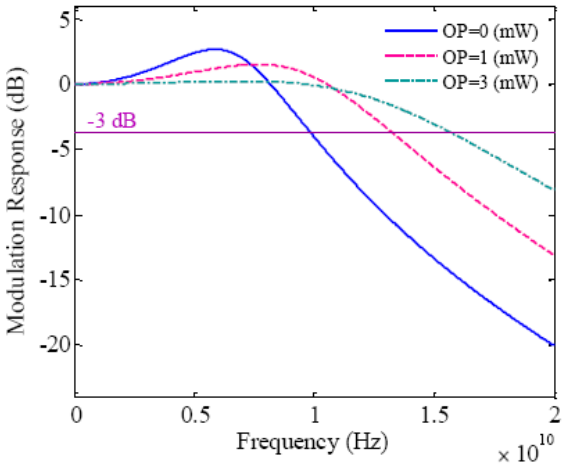

Fig. 4 Modulation response of QD laser for three different values of optical pumping and at *I*=55mA. Optical pump makes the modulation response of QD laser wider and increases its 3dB bandwidth.

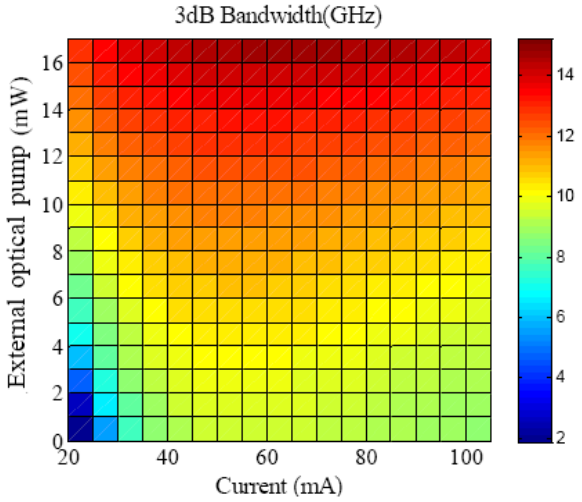

Fig. 5 The 3dB bandwidth of QD laser versus current and optical pump power. External optical beam helps to modulate the laser electrically at lower bias currents with higher frequencies.

In Figs. 6(a-d), the turn-on dynamics of carriers and photons have been plotted for a step current from zero to *I*=55mA. As shown, the number of carriers at all three states of WL, ES, and GS grow during shorter delay time by increasing the external optical pump. Actually, by injecting carriers to the ES through optical pump, the carrier flow between the WL and QDs' states also grows and hence the WL carrier population reaches to its steady state point at higher speed similar to the ES and GS carriers. Furthermore, the output power of QD laser also would turn on during shorter delay time with increasing optical pump which is in confirmation with the previous results for modulation response [9].

The delay time of QD laser as a function of bias current at three different values of optical pump power is shown in Fig. 7. Calculations imply that the turn-on delay time of QD laser decreases by driving the laser at higher currents. Moreover, external optical beam decreases the value of delay time significantly. From physical viewpoint, feeding the ES with excess carriers acts as an internal compensator in system of carriers and photons and hence causes the GS carriers and photons to reach their steady state values during shorter time.

[Downloaded from ijop.ir on 2026-11-25]

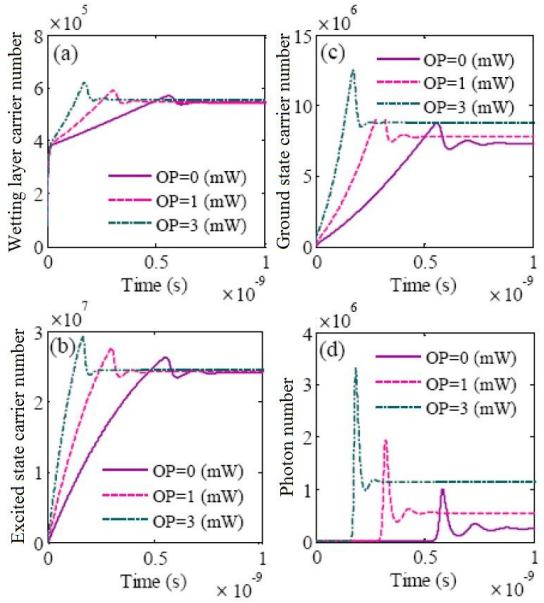

Fig. 6 Turn-on dynamics of carriers and photons for a step current from zero to *I*=55mA. The number of carriers at all three states of the (a) WL, (b) ES, and (c) GS and also (d) photons grow during shorter delay time by increasing the external optical pump.

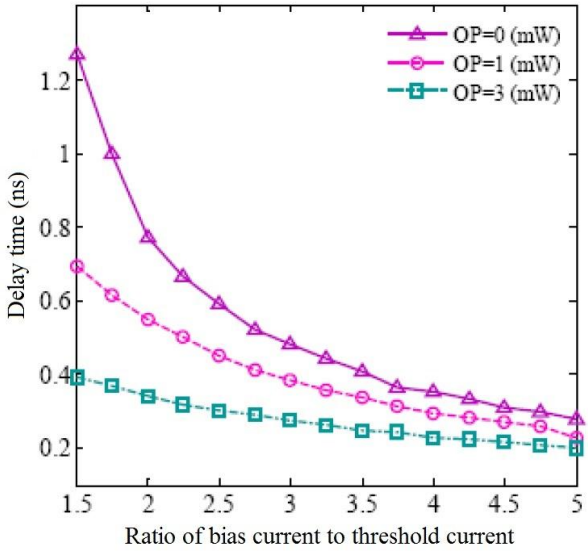

Fig. 7 The delay time of QD laser versus current under three different optical pump powers. External optical beam decreases the value of delay time significantly.

In Fig. 8, the RIN spectrum of InAs/InP QD laser is plotted for three different values of optical pumping and at the injection current of *I*=55mA.

It is depicted that the RIN spectrum in all three cases has a level between -145 and -160dB/Hz at different frequencies till the resonance frequency which moves toward higher frequencies under higher optical pumping. Furthermore, external optical beam decreases the RIN level and increases the damping factor. In fact, it is evident that external optical beam raises the number of carriers and photons and hence makes the GS carriers and photons to relatively become more stable. Therefore, this stability of carriers and photons due to optical pump leads to lower relative fluctuations and thus lower intensity noise.

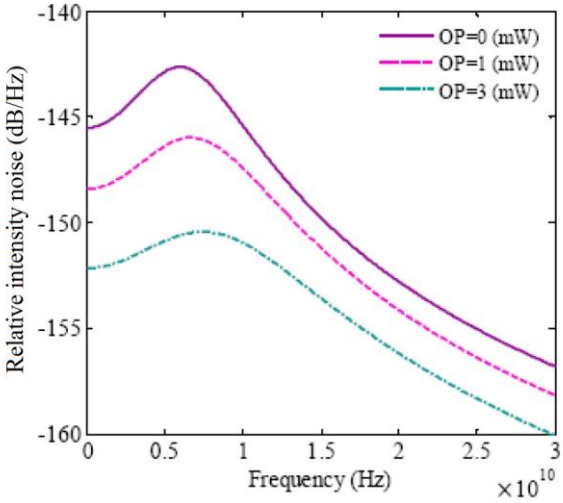

Fig. 8 The relative intensity noise spectrum of InAs/InP QD laser for three different values of optical pumping and at the injection current of *I*=55mA. External optical beam decreases the level of RIN and increases the damping factor.

Further, we have divided auto and cross correlation terms of different carrier and photon reservoirs into three groups, called as the WL, quantum, and photon noises separately. In Fig. 9, the values of three aforementioned noises are plotted versus current at f=1GHz, for three different optical pump powers.

It is shown that the levels of all intensity fluctuations decrease through increasing the bias current while the photon and quantum noise sources play the dominant role in overall value of RIN in QD lasers. Moreover, it is deduced that by increasing external optical beam, the values of these shot noise sources reduce at all bias points.

Based on the phase rate equation, the central frequency of QD laser shows some shifts

[Downloaded from ijop.ir on 2026-11-25]

under steady state conditions. This frequency chirping is the natural result of the refractive index change which depends on the carriers' populations [27]. In Fig. 10, we have plotted the steady state frequency chirp of QD laser, relative to the central frequency $((\omega_L - \omega_0)/\omega_0)$, for three different optical pump powers.

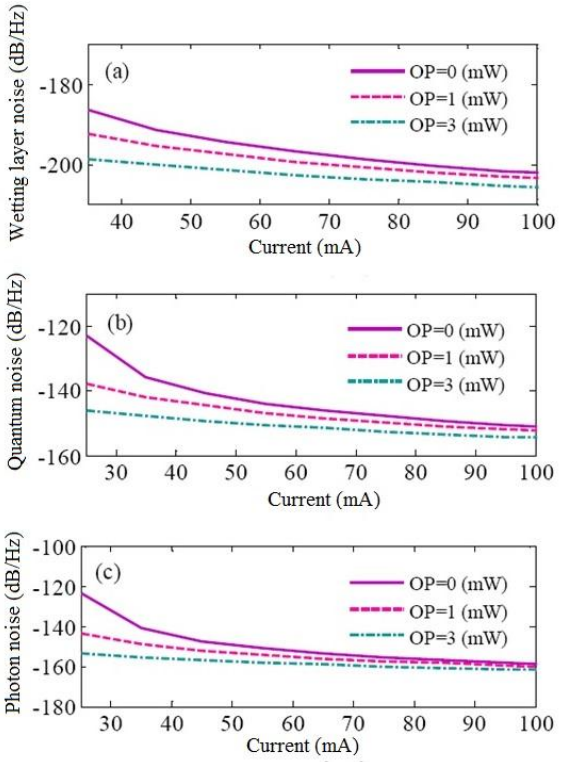

Fig. 9 The values of the (a) WL, (b) quantum, and (c) photon noises versus current at f=1GHz for three different optical pump powers. External optical beam reduces the values of three shot noise sources at all bias points.

It is depicted that the absolute value of the frequency chirp has descending trend by increasing the current above threshold and the external optical pump leads to lower frequency chirp. Comparing refractive index changes due to interband transitions and free carrier absorption, it is found that the first one plays the essential role on overall value of the refractive index changes and therefore on the steady state frequency chirping in QD lasers. From physical viewpoint, by increasing the pumping, the carriers' populations reach their final value and therefore get more stable which in turn leads to lower refractive index changes. Furthermore, the frequency shift has always negative values and thus the laser beam shows red shift at higher output powers.

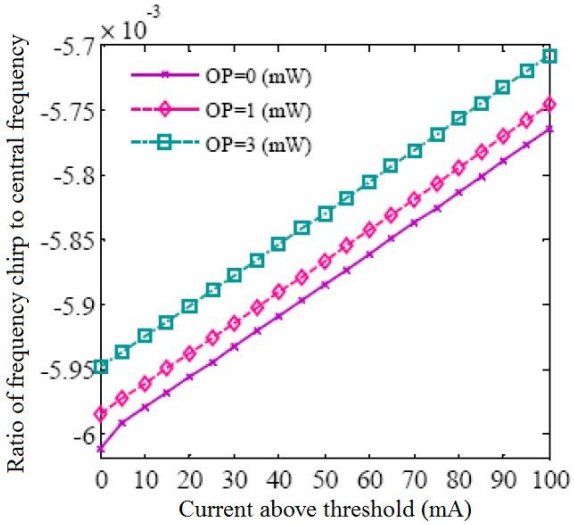

Fig. 10 The steady state frequency chirp of QD laser relative to the central frequency at three different optical pumping.

To investigate the impact of external optical pumping on the frequency noise spectrum of QD laser, we have plotted the FN spectrum for three different optical pump powers and at I=55mA in Fig. 11.

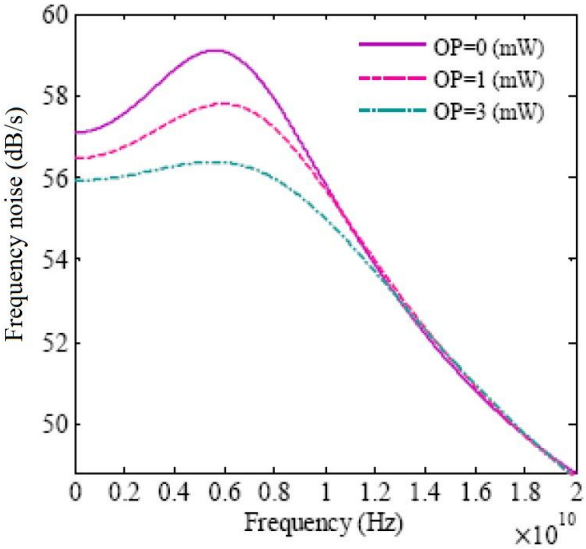

Fig. 11 The frequency noise spectrum of QD laser for three different optical pump powers and at the injection current of I=55mA. The FN level reduces and the resonant frequency grows at higher optical pumps.

It is shown that by increasing the optical pump and thus the output power, the frequency noise

[Downloaded from ijop.ir on 2026-11-25]

level reduces and the resonant frequency of QD laser moves toward larger values. Similar behavior is also observed in the relative intensity noise spectrum of QD lasers. From physical point of view, through external optical pump, the populations of the ES and GS carriers grow at the operation point and hence the relative carrier fluctuations decrease around this point.

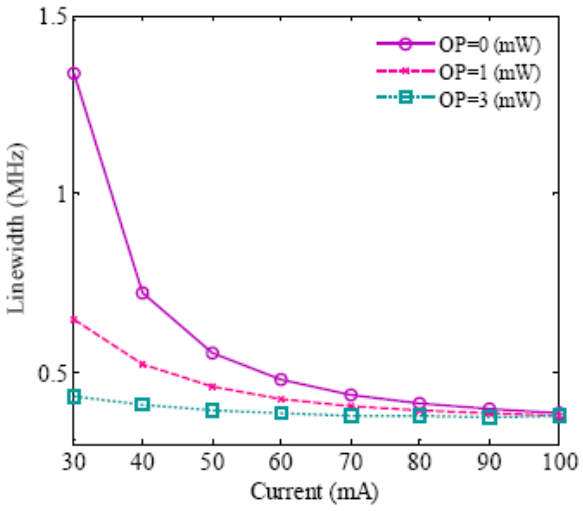

Fig. 12 The linewidth of QD laser versus current at three different values of optical pump power. Under external optical beam, the linewidth of QD laser decreases and reaches the values lower than 700 kHz.

From frequency noise calculations, we can evaluate the linewidth of QD laser under small signal modulations [21]. In Fig. 12, the linewidth of QD laser has been plotted as a function of current at three different values of optical pump power. It is depicted that the linewidth of QD laser decreases with increasing the output power by raising either the current or optical pumping level. Furthermore, it is evident that by external optical beam, the linewidth of QD laser decreases even at zero bias current and reaches the values lower than 700 kHz which is more favorable for high speed modulation applications.

IV. Conclusion

The impacts of external optical pumping on the modulation response, relative intensity noise and frequency noise characteristics of nonlinear 1.55μm QD lasers have been inspected theoretically. The small signal analysis of the rate equations for the carriers and photon numbers reveals that the modulation response of QD laser enhances in the presence of an external optical beam. Actually, it is deduced that by injecting excess carriers directly to the ES via optical pumping, the 3dB bandwidth of the laser increases. The external optical beam also causes the turn-on delay time to be reduced significantly. Moreover, calculations imply that the RIN level of QD laser decreases and the damping factor increases due to the external beam. It is also demonstrated that by increasing the external optical pump, the FN level of QD laser decreases which leads to lower linewidth under small signal modulation. In summary, it is concluded that by applying a low power optical pump to the ES of QD laser, its dynamic response and intensity and frequency noise characteristics could be improved significantly.

References

[1] D. L. Huffaker, G. Park, Z. Zou, O. B. Shchekin, and D. G. Deppe, “1.3 μm Room-Temperature GaAs-Based Quantum-Dot Laser," Appl. Phys. Lett. Vol. 73, no. 18, pp. 2564-2566, 1998.

[2] L. Drzewietzki, G. A.P. Thè, M. Gioannini, S. Breuer, W. Elsäßer, M. Hopkinson, M. Krakowski, and I. Montrosset, “Theoretical and Experimental Investigations of The Temperature Dependent Continuous Wave Lasing Characteristics and The Switch-On Dynamics of An InAs/InGaAs Quantum-Dot Semiconductor Laser,” Opt. Commun., vol. 283, no. 24, pp. 5092-5098, 2010.

[3] T. J. Badcock, R. J. Royce, D. J. Mowbray, M. S. Skolnick, H. Y. Liu, M. Hopkinson, K. M. Groom, and Q. Jiang, “Low Threshold Current Density And Negative Characteristic Temperature 1.3 μm InAs Self-Assembled Quantum Dot Lasers,” Appl. Phys. Lett., vol. 90, no. 11, pp. 111102.1-111102.3, 2007.

[4] P. F. Xu, T. Yang, H. M. Ji, Y. L. Cao, Y. X. Gu, Y. Liu, W. Q. Ma, and Z. G. Wang, “Temperature-Dependent Modulation Characteristics For 1.3μm InAs/GaAs

[Downloaded from ijop.ir on 2026-11-25]

Quantum Dot Lasers," J. Appl. Phys., vol. 107, no. 1, pp. 013102.1-013102.5, 2010.

[5] P. M. Smowton, S. N. Elliott, S. Shutts, M. S. Al-Ghamdi, and A. B. Krysa, "Temperature-Dependent Threshold Current in InP Quantum-Dot Lasers," IEEE Selec. Topics Quantum Electron., vol. 17, no. 5, pp. 1343-1348, 2011.

[6] S. G. Li, Q. Gong, C. F. Cao, X. Z. Wang, P. Chen, L. Yue, Q. B. Liu, H. L. Wang, C. H. Ma, "Temperature Dependent Lasing Characteristics Of InAs/InP(100) Quantum Dot Laser," Mat. Sci. Semic. Proc., vol. 15, no. 1, pp. 86-90, 2012.

[7] Z. J. Jiao, Z.G. Lu, J.R. Liu, P.J. Poole, P.J. Barrios, D. Poitras, J. Caballero, X.P. Zhang, and G. Pakulski, "Linewidth Enhancement Factor of InAs/InP Quantum Dot Lasers Around 1.5 μm," Opt. Commun., vol. 285, no. 21, pp. 4372-4375, 2012.

[8] K. C. Kim, K. Han, Y. C. Yoo, J. Lee, Y. M. Sung, and T. G. Kim, "Optical Characteristics And The Linewidth Enhancement Factor Measured from InAs/GaAs Quantum Dot Laser Diodes," IEEE Trans. Nanotech., vol. 7, no. 2, pp. 135-139, 2008.

[9] D. Gready, G. Eisenstein, V. Ivanov, C. Gilfert, F. Schnabel, A. Rippien, J. P. Reithmaier, and C. Bornholdt, "High Speed 1.55 μm InAs/InGaAlAs/InP Quantum Dot Lasers," IEEE Photon. Technol. Lett., vol. 26, no. 1, pp. 11-13, 2014.

[10] D. Gready, G. Eisenstein, H. Schmeckebier, M. Gioannini, M. Stubenrauch, I. Montrosset, D. Arsenijevic, and D. Bimberg, "On the Relationship between Small and Large Signal Modulation Capabilities in Highly Nonlinear Quantum Dot Lasers," Appl. Phys. Lett., vol. 102, no. 10, pp. 101107 (1-3), 2013.

[11] K. Lüdge, M. J. P. Bormann, E. Malic, P. Hovel, M. Kuntz, D. Bimberg, A. Knorr, and E. Schöll, "Turn-On Dynamics And Modulation Response In Semiconductor Quantum Dot Lasers," Phys. Rev. B, vol. 78, no. 3, pp. 035316. (1-3), 2010.

[12] F. Grillot, B. Dagens, J. G. Provost, H. Su, and L. F. Lester, "Gain Compression and Above-Threshold Linewidth Enhancement Factor in 1.3-μm InAs–GaAs Quantum-Dot Lasers," IEEE J. Quantum Electron., vol. 44, no. 10, pp. 1144-1149, 2008

[13] C. Wang, F. Grillot, and J. Even, "Impacts of Wetting Layer and Excited State on the Modulation Response of Quantum-Dot Lasers," IEEE J. Quantum Electron., vol. 48, no. 9, pp. 1144-1149, 2012.

[14] B. Lingnau, K. Ludge, W. W. Chow, and E. Schöll, "Influencing Modulation Properties Of Quantum-Dot Semiconductor Lasers By Carrier Lifetime Engineering," Appl. Phys. Lett., vol. 101, no. 13, pp. 131107 (1-4), 2012.

[15] S. Bhowmick, M. Z. Baten, T. Frost, B. S. Ooi, and B. Bhattacharya, "High Performance InAs/$InGa_{0.53}Al_{0.23}As_{0.24}$/InP Quantum Dot 1.55μm Tunnel Injection Laser," IEEE J. Quantum Electron., vol. 50, no. 1, pp. 7-14, 2014.

[16] K. Lüdge, and E. Schöll, "Nonlinear Dynamics of Doped Semiconductor Quantum Dot Lasers," Eur. Phys. J. D, vol. 58, no. 2, pp. 167-174, 2010.

[17] Y. Li, N. A. Naderi, V. Kovanis, and L. F. Lester, "Enhancing the 3-dB Bandwidth via the Gain Lever Effect in Quantum Dot Lasers," IEEE J. Photon., vol. 2, no. 3, pp. 321-329, 2010.

[18] M. C. Pochet, N. A. Naderi, V. Kovanis, and L. F. Lester, "Modeling the Dynamic Response of an Optically-Injected Nanostructure Diode Laser," IEEE J. Quantum Electron., vol. 47, no. 6, pp. 827-833, 2011.

[19] C. Wang, B. Lingnau, K. Lüdge, J. Even, and F. Grillot, "Enhanced Dynamic Performance of Quantum Dot Semiconductor Lasers Operating on the Excited State," IEEE J. Quantum Electron., vol. 50, no. 9, pp. 723-731, 2014.

[20] F. Grillot, K. Veselinov, M. Gioannini, I. Montrosset, J. Even, R. Piron, E. Homeyer, and S. Loualiche, "Spectral Analysis of 1.55μm InAsInP(113)B Quantum-Dot Lasers Based on a Multipopulation Rate Equations Model," IEEE J. Quantum Electron., vol. 45, no. 7, pp. 872-878, 2009.

[21] G. P. Agrawal and N. K. Dutta, *Semiconductor Laser*s, 2nd ed., New York: Van Nostrand Reinhold, 1993.

[22] J. Pausch, C. Otto, E. Taylaite, N. Majer, E. Schöll, and K. Lüdge, "Optically injected quantum dot lasers: impact of nonlinear carrier lifetimes on frequency-locking dynamics,"

[Downloaded from ijop.ir on 2026-11-25]

New J. Phys., vol. 14, no. 5, pp. 053018-053020, 2012.

[23] A. Sahraee and A. Zarifkar, "Gain and Phase Dynamics of QD-VCSOA under Electrical and Optical Pumping," IEEE J. Lightwave Technol., vol. 32, no. 22, pp. 4318-4325, 2014.

[24] M. Sanaee, and A. Zarifkar, "Theoretical Modeling of Relative Intensity Noise in p-doped 1.3μm InAs/GaAs Quantum Dot Lasers," IEEE J. Lightwave Technol. Vol. 33, no. 1, pp. 234-243, 2015.

[25] M. Sanaee and A. Zarifkar, "Effect of carrier transition mechanisms and gain compression on relative intensity noise of 1.55 μm QD lasers," Opt. Commun.**,** vol. 353, pp. 42-48, 2015.

[26] L. A. Coldren, S. Corzine, and M. Mashanovitch, *Diode lasers and photonic integrated circuits*, 2nd ed., New Jersey : J. Wiley & Sons, 2012.

[27] M. Sanaee, A. Zarifkar, and M. H. Sheikhi, "Frequency Noise Analysis of 1.55μm InAs/InP QD Lasers: Impact of Nonlinear Gain and Direct Carrier Transition," IET Optoelectron., vol. 10, no. 4, pp. 134-141, 2016.



Maryam Sanaee received the B.Sc. (Hons.), M.Sc., and Ph.D degrees in electrical engineering from Shiraz University, Shiraz, Iran, in 2007, 2010 and 2015, respectively. Her research interests include simulation and modeling of photonic devices, nanoelectronics devices, and quantum computation.



Abbas Zarifkar received the B.Sc. degree from Shiraz University, Shiraz, Iran, in 1992, and the M.Sc. and Ph.D. degrees from Tarbiat Modares University, Tehran, Iran, in 1995 and 2001, respectively, all in electrical engineering. He was the head of the optical communications group at Iran Telecommunication Research Center (ITRC) from 2004 to 2007, and a member of the board of Telecommunication Infrastructure Company of Iran from 2006 to 2007, Tehran. He was the deputy director for research and development at the ITRC and the director of the ITRC from 2007 to 2009. He is currently an associate professor at the Faculty of Electrical and Computer Engineering, Shiraz University. His research interests include the modeling and simulation of optoelectronic devices, noise in optical devices, DWDM components and systems, and design of optical communication systems. He was selected as the distinguished researcher in the field of information and communication technology in 2005.

[Downloaded from ijop.ir on 2026-11-25]

THIS PAGE IS INTENTIONALLY LEFT BLANK.

[Downloaded from ijop.ir on 2026-11-25]